All-Silica Colloidosomes with a Particle-Bilayer Shell

Hailin Wang, Xiaomin Zhu,* Larisa Tsarkova, Andrij Pich, and Martin Möller

DWI an der RWTH Aachen e.V. and Institute for Technical and Macromolecular Chemistry of RWTH Aachen University, Pauwelsstrasse 8, D-52056 Aachen, Germany

ABSTRACT We report on the preparation of all-silica colloidosomes with adjustable size, shell structure, mechanical strength, and permeability. Our approach is based on the coassembly at the water/oil interface of silica nanoparticles and a silica precursor polymer—hyperbranched polyethoxysiloxane—which acts as a binder for particles as well as an additional interfacial component. Remarkably, the shell of colloidosomes can be fine-tuned from a particle monolayer up to a bilayer bound with a sandwiched thin silica film. This method presents a facile approach toward multiscale production of microcapsules which have a high potential in encapsulation technology and in smart coating formulations.

KEYWORDS: silica · colloidosome · Pickering emulsion · bilayer · self-assembly · sol–gel process

Solid colloidal particles can be strongly attached to fluid interfaces[1] and are known to stabilize oil–water emulsions.[2,3] These so-called Pickering emulsions have been used to fabricate microcapsules by fixing the particle assemblies at an interface using different strategies including electrostatic binding with polyelectrolytes,[4,5] van der Waals interactions,[4,5] sintering,[5,6] gelation,[7,8] chemical cross-linking,[9–12] and polymerization.[13] The capsules prepared in this way are called colloidosomes by analogy with liposomes.[5] They show a high potential in a number of technological applications related to encapsulation techniques and to formulations of smart coatings. The application of the colloidosomes strongly relies on facile and low-cost preparation methods allowing tunable characteristics such as wall thickness, rigidity, porosity, as well as chemical composition. These structural features are essential for controlled release of encapsulated materials.

The interfacial assembly of colloidal particles was intensively studied experimentally[4,14–17] as well as theoretically.[18–21] This assembling process is driven by a decrease in total free energy upon the placement of a particle at the fluid/fluid interface. The build-up of a monolayer of particles or particle aggregates at the interface has been proved *ex situ* by scanning force microscopy and transmission electron microscopy (TEM) and *in situ* by grazing-incidence small-angle X-ray scattering technique.[22] The formation of a double particle layer was theoretically predicted[21] and experimentally evidenced[17] at a planar air/oil/water interface, that is, in a system involving two interfaces. This scenario, however, can be achieved only in a narrow window of interfacial energies, and is considered as the formation of two monolayers rather than a bilayer. The assembly of a particle bilayer in a Pickering emulsion remains an experimental challenge. Up to now, the reported colloidosomes consist mostly of a monolayer[4–13] or a very thick multilayer particle shell (in the case of double emulsion).[23] Accordingly, the shell permeability in colloidosomes is generally adjusted by varying the particle size.

Here, we present a simple method for the preparation of silica colloidosomes with a shell that can be fine-tuned from a particle monolayer up to a well-defined bilayer. In our approach, a silica precursor polymer—hyperbranched polyethoxysiloxane (PEOS)[24]—is added as an interfacial "glue" to a water-in-oil (w/o) Pickering emulsion stabilized by silica nanoparticles. We study systematically the influence of the interfacial sol–gel reaction conditions on the structure of the colloidosomes, and subsequently their release properties.

RESULTS AND DISCUSSION

Our approach for the production of silica colloidosomes is outlined in Figure 1. In this procedure, the w/o Pickering emulsion stabilized by silica nanoparticles serves as a template for capsules. Nearly monodisperse silica nanoparticles with an average diameter of 50 nm were prepared by the Stöber method,[25] and they were hydrophobized using octadecyltrimethoxysilane. The modification degree was carefully adjusted in such a way that the particles effectively stabilized a w/o emulsion, while a portion

* Address correspondence to zhu@dwi.rwth-aachen.de.

Received for review February 2, 2011 and accepted March 31, 2011.

Published online March 31, 2011
10.1021/nn200436s

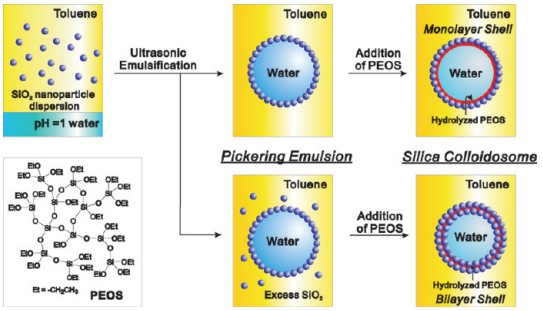

Figure 1. Schematic illustration of the formation of silica colloidosomes and the chemical structure of hyperbranched polyethoxysiloxane (PEOS).

of free silanol groups were still available at the particle surface for the reaction with PEOS. The Pickering emulsion was prepared by mixing a particle dispersion in toluene with an HCl aqueous solution (at pH = 1) under ultrasonic emulsification. Afterward, a toluene solution of PEOS was added. In this system, the volume ratio of toluene to water and the PEOS concentration were fixed to 10:1 and 0.012 g·mL^{-1}, respectively. The emulsion was gently stirred for 3 days allowing the full conversion of PEOS. The resulting colloidosomes were isolated by centrifugation. We note that after isolation they can still be redispersed in nonpolar solvents such as toluene, hexane, *etc.* The colloidosome dimensions and the shell structure were analyzed by TEM, scanning electron microscopy (SEM), fluorescence microscopy, and FT-IR spectroscopy. Thermogravimetric analysis (TGA) was used to probe the permeability of water across the shell of these capsules.

The most important observation is the formation of a capsular shell composed of a well-defined particle bilayer bound with a sandwiched thin silica film. The transition from a monolayer to a bilayer takes place at the excess of silica nanoparticles in the emulsion (Figure 1).

Figure 2 shows typical microscopic images of the obtained colloidosomes. The fluorescence micrograph (Figure 2a) depicts toluene-dispersed colloidosomes prepared using an aqueous solution of a fluorescent dye tris(2,2′-bipyridyl)dichlororuthenium(II) hexahydrate (Ru(bpy)), and the capsular structure is clearly confirmed. Most colloidosomes are spherical with dimensions ranging from several hundred nanometers to several micrometers. The electron micrographs in Figure 2b provide the view of the capsules in the dry state and reveal the details of their shell structure: in the colloidosome shell the silica nanoparticles are close-packed with a nearly hexagonal symmetry, and a 10−15 nm thick continuous layer in the shell is clearly visible. Comparison of FT-IR spectra of the resulting colloidosomes in the dry state with that of PEOS and the initial silica nanoparticles (Figure 3) strongly indicates that PEOS is fully converted and that the colloidosomes almost entirely consist of silica. Therefore, we

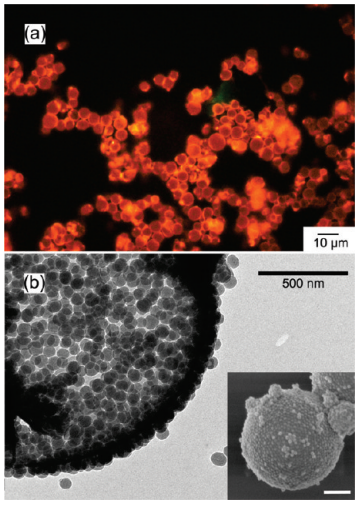

Figure 2. Microscopic images of typical colloidosomes. (a) Fluorescence micrograph of a toluene dispersion of colloidosomes with an encapsulated aqueous solution of a fluorescent dye Ru(bpy); (b) TEM and SEM (inset, the bar represents 500 nm) images of colloidosomes in the dry state.

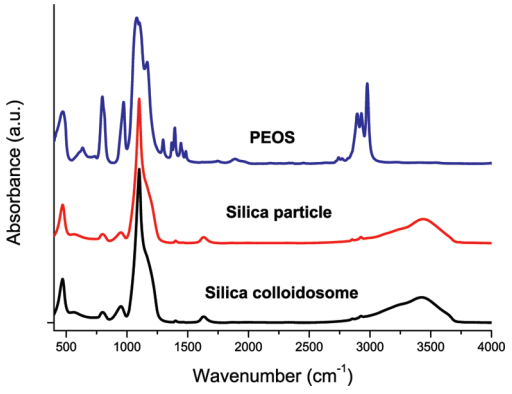

Figure 3. FT-IR spectra of PEOS, silica nanoparticles, and dried silica colloidosomes.

believe that the thin continuous layer comprises silica formed from PEOS. Moreover, simple calculations confirm this statement. The thickness of the PEOS layer as derived from the preparation procedure is 30−45 nm. Upon conversion, the PEOS layer loses *ca.* 50% weight by eliminating ethanol. At the same time, its density changes from 1.14 g·cm^{-3} for PEOS to 1.65 g·cm^{-3} for hydrated silica.[26] Thus, the detected thickness of the silica layer (10−15 nm) is in good agreement with the initial PEOS content.

In the TEM image (Figure 2b) the silica layer produced by acidic hydrolysis and condensation of PEOS appears more transparent toward an electron beam than the silica particles due to lower density and smaller thickness of the former. As seen in the electron micrographs, most colloidosomes sustained the spherical morphology without collapse even under high vacuum and high voltage electron irradiation, indicating an enhanced mechanical strength.

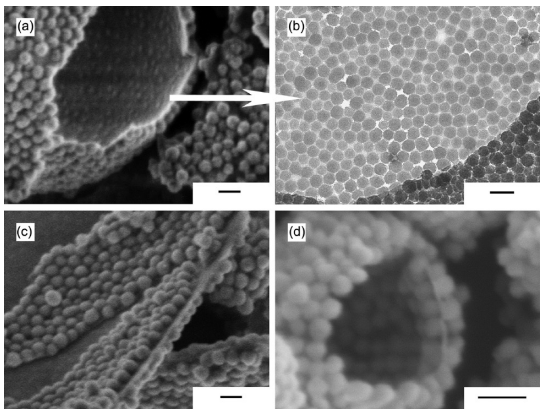

Figure 4. Scanning (a, c, d) and transmission (b) electron micrographs of silica colloidosomes with a particle monolayer (a, b) and a bilayer (c, d) shell structure. The bars represent 100 nm.

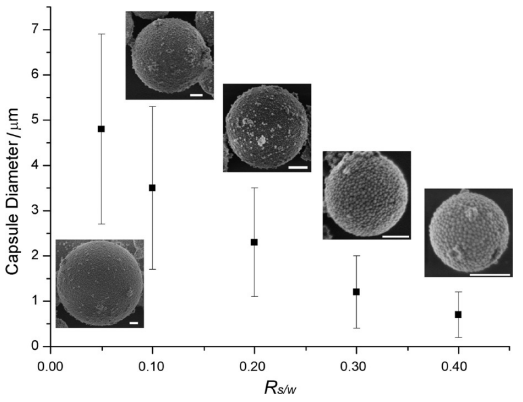

Figure 5. The influence of the weight ratio of silica nanoparticles to water ($R_{s/w}$) on the capsule size. The insets are the corresponding SEM images of typical colloidsomes. The bar represents 500 nm. The volume fraction of toluene to water is 10:1, and the concentration of PEOS in toluene is 0.012 g·mL^{-1}.

Figure 4 displays the cross-sectional views of colloidosomes with a particle monolayer (Figure 4a,b) and a bilayer structure (Figure 4c,d). The SEM image of an "opened" monolayer capsule (Figure 4a) confirms that in this case the inner surface of the shell is free from particles and is relatively smooth. For colloidosomes with a bilayer shell, the solidified PEOS layer is also clearly visible. The outer surface of the shell is always fully covered by the colloidal particles, but the inner side can be partially (Figure 4c) or fully (Figure 4d) occupied by the particles. On the partially covered inner surface, the particles are assembled into hexagonally close-packed arrays with no isolated particles in the vicinity (Figure 4c). At a constant toluene/water ratio and PEOS concentration, the shell structure of colloidosomes can be tuned by varying the weight ratio of silica nanoparticles to water ($R_{s/w}$). At $R_{s/w} < 0.05$, Pickering emulsions are still formed, but no colloidosomes can be obtained. We attribute this observation to loose particle coverage of the emulsion interface which prevents the nanoparticles from acting as scaffolds for capsules. The colloidosomes are formed starting from $R_{s/w} \approx 0.05$. At $R_{s/w} = 0.05$, the colloidosomes have a particle monolayer shell (Figure 4a,b). A second layer of particles on the inner surface appears with the further increase of $R_{s/w}$ (Figure 4c,d). We note that the above-described transition to a complete bilayer shell occurs at $R_{s/w} \approx 0.40$ (Figure 4d). In this case, as evidenced by almost 100% integrity of the capsules after the drying procedure, they possess an enhanced rigidity, most probably both due to more robust shell and due to their smaller size. Figure 5 demonstrates the dependence of the colloidosome dimension *versus* $R_{s/w}$. As expected, the size decreases gradually from 4.8 ± 2.1 to 0.7 ± 0.5 μm with the increase of $R_{s/w}$ from 0.05 to 0.4 (Figure 5), suggesting a better dispersion of the water phase in toluene at high $R_{s/w}$.

Further we address the mechanism of the interfacial assembly of particles and PEOS molecules. Systematic studies on the effect of the PEOS concentration on the formation of colloidosomes (at a defined toluene/water ratio) revealed an optimal PEOS concentration of 0.012 g·mL^{-1} in toluene which was kept constant throughout this study. At higher PEOS concentrations, the emulsion breaks down, presumably due to the destructive effect of the reaction product—ethanol—on the emulsion stability.[27] Lower PEOS concentrations (<0.012 g·mL^{-1}) are possibly not sufficient to build a mechanically stable shell from converted PEOS and nanoparticles.

The interfacial sol–gel reaction of PEOS plays a pivotal role in the formation of monolayer and bilayer shells. Because of high incompatibility between PEOS and water, the hydrolysis takes place only at the w/o interface. It was earlier demonstrated that PEOS does not wet the water surface at the initial stage of the contact.[28] During the hydrolysis, the solubility of PEOS in hydrocarbon is reduced and its affinity to water increases. Therefore, the structure of hydrolyzed PEOS resembles that of the amphiphilic surfactant molecules. As a result, a wetting layer of hydrolyzed PEOS is gradually formed between water and oil. This enables the PEOS droplets to spread until the liquid phase is transformed into a solid film.[28] The interfacial sol–gel reaction under acidic conditions is a relatively slow process; it takes 3 days to fully convert PEOS to a thin silica film at pH 1. During this time hydrolyzed PEOS layer remains liquid.

As a result of the condensation reaction between the ethoxysilane or silanol groups of PEOS and the surface silanol groups of silica nanoparticles, PEOS acts as a binder for the silica nanoparticles at the interface. Shown in Figure 6a are capsules obtained after one day of the sol–gel reaction, and they exhibit a soft nature and limpness. Inset in Figure 6a shows an example of noncomplete coverage of the inner shell surface at this reaction stage. It is likely that the particle

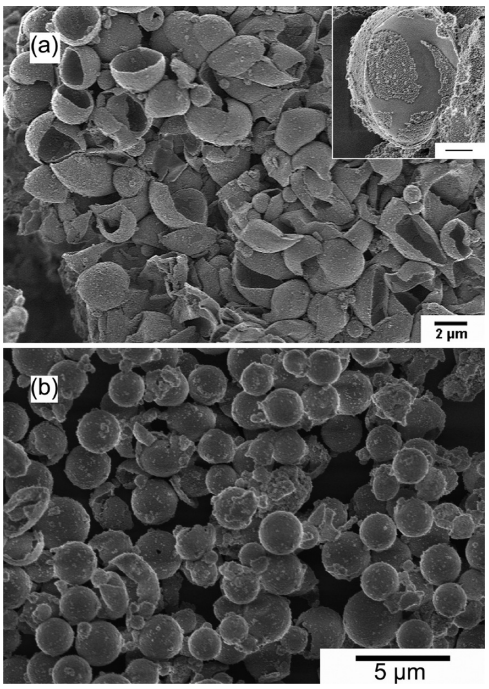

Figure 6. SEM images of colloidosomes after 1 day (a) and 3 days (b) of sol−gel reaction. The inset in panel a shows the drift of particle assemblies on the colloidosome inner surface (the bar represents 500 nm).

assemblies were detached from a larger piece and drifted apart to their current positions. This is an important indication that at this stage the partially hydrolyzed PEOS layer is still liquidlike. PEOS molecules continuously migrate to the water surface and cleave the nanoparticle array. In contrast to the shorter reaction time, colloidosomes which are isolated after the full conversion retain their integrity after drying and possess a high hardness (Figure 6b).

Because the hydrolysis of PEOS is pH sensitive, we established optimal water phase pH values for the colloidosome formation. In the pH range of 1−4, the whole process is pH insensitive, and colloidosomes with similar morphology are obtained. Given that the hydrolysis of alkoxysilane groups at low pH is faster than the condensation[29] and the access to water is limited at the interface, the hydrolyzed PEOS layer remains liquid for three days. At pH = 6, the colloidosome surface is covered with fragmented particle aggregates rather than with a homogeneous particle layer. At pH above 6, the condensation becomes dominant over the hydrolysis,[29] so the reaction of PEOS with water leads to the formation of particles instead of branched and weakly cross-linked polymer chains as in the case of acidic catalysis. Therefore, at high pH values PEOS does not function as an interfacial linker of silica particles, and colloidosomes are not formed.

On the basis of the above results, we conclude that the formation of silica colloidosomes involves three steps including the formation of w/o Pickering emulsions, hydrolysis of PEOS at the water interface with the reassembly of nanoparticles, and PEOS solidification. Among these steps, the second one is crucial for the structure formation of the final colloidosomes. At this stage, a toluene/PEOS/water/particle quaternary emulsion system is formed. As the fourth component (hydrolyzed PEOS) is involved in the emulsion system, new interfaces emerge. Silica nanoparticles then move from the water/toluene to the toluene/PEOS interface. If the amount of silica nanoparticles is sufficient, they occupy also the PEOS/water interface. This can be explained as follows. The silica particles are hydrophobic because of the hydrocarbon coating; they preferably stabilize the hydrophilic-in-hydrocarbon emulsion (hydrolyzed PEOS-in-toluene) rather than hydrophilic-in-hydrophilic (water-in-hydrolyzed PEOS) system.[20] This gives the reason for the observation that the outer surface of the colloidosome shell is always fully covered by particles and only at high $R_{s/w}$ are the particles located on the inner surface. Because of the capillary force, the particles on the inner side of the shell assemble to pieces rather than reside separately. Therefore, the assembling of the nanoparticles at the toluene/hydrolyzed PEOS/water interface is attributed to the interplay of surface energies in a complex quaternary interfacial system. The successful formation and stabilization of colloidosomes is extremely sensitive to the system composition such as the particle and PEOS concentrations, surface properties of silica nanoparticles, *etc.*, as well as to the external conditions (pH and time).

The colloidosomes prepared in this work are composed almost entirely of inorganic silica phase. To probe the barrier properties of the capsules, we conducted dye release experiments in which the colloidosomes with an encapsulated aqueous solution of a fluorescent dye were isolated and placed into water. Two dyes, namely Ru(bpy) and sulforhodamine B sodium salt, were tested, and in both cases no fluorescence was detected in the external medium even after 30 days. We attribute this result to the compact and hydrophobic nature of the capsular shell.

Further, our all-silica colloidosomes have other clear advantages over the organic and hybrid materials. First, the incorporated ingredient is expected to be released under mechanical force due to the brittleness of the pure silica. Second, because of the high thermal stability and chemical resistance of silica, these colloidosomes can be used to encapsulate highly aggressive fluids such as an aqueous solution of hydrogen peroxide.

To exploit the potential in controlled release applications, we used TGA to study the stability and permeability of the colloidosomes. Figure 7a displays the weight loss under isothermal conditions of the samples prepared at varied $R_{s/w}$ values. Importantly, the total weight loss upon heating is close to the amount of water used in the preparation of the colloidosomes.

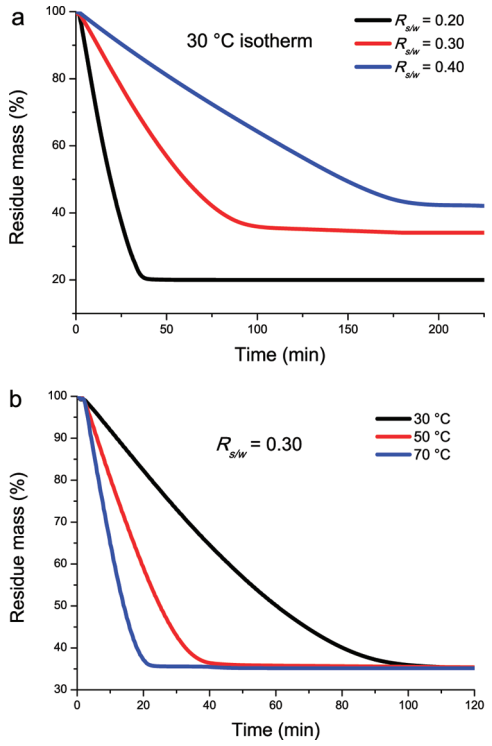

Figure 7. Evaporation of encapsulated water from colloidosomes under isothermal conditions. (a) Colloidosomes prepared with different $R_{s/w}$ and TGA measurement carried out at 30 °C; (b) colloidosomes prepared at $R_{s/w}$ = 0.30 and TGA measurement carried out at different temperatures.

The SEM images of the residue after the water evaporation (not shown) reveal no change in the morphology, implying that water molecules escape from the colloidosomes through nanopores without destroying the capsules. The data demonstrate that the water evaporation rate can be controlled by $R_{s/w}$, that is, by the thickness as well as the averaged density of the silica shell, and it can be significantly slowed down by densely packed bilayer morphology. Smaller water droplets evaporate normally faster than the larger ones because of the larger specific surface area. However, due to the differences in the shell structure, the encapsulated water in smaller capsules has a lower evaporation rate than that in bigger ones. We attribute the observed permeability properties of the capsules to the high degree of nanoporosity of the thin silica layer obtained by PEOS condensation.[28] Such a structure allows small molecules like water vapor to diffuse across the shell. In the bilayer shell the second particle layer on the inner surface reduces the contact area of the thin silica layer with water, hence, improving the barrier properties. Figure 7b presents the weight loss at various temperatures, and it shows that the evaporation rate expectedly increases with increasing temperature. Thus, in this work we managed to control the release rate of small molecules by tuning the shell structure from a monolayer to a bilayer of particles. This opens a facile route toward design and adjustment of barrier properties of such capsules.

CONCLUSION

For the first time colloidosomes with a controllable shell structure and a tunable size have been developed using a water/toluene emulsion stabilized by partially hydrophobized silica nanoparticles as a template in combination with a liquid polymeric silica precursor PEOS as a binder. A mechanism based on an interfacial sol–gel process has been proposed to explain the formation of a particle monolayer and bilayer. We demonstrated that the evaporation rate of the encapsulated water can be controlled by the shell structure of the colloidosomes. This technique opens a new gateway for the design of functional inorganic microcapsules.

EXPERIMENTAL SECTION

Preparation of Hydrophobic Silica Nanoparticles. Tetraethoxysilane (1.67 mL, 98%, Aldrich) and ammonia aqueous solution (25%, 2.5 mL, KMF) were dissolved in absolute ethanol (50 mL, VWR). The mixture was kept under gentle stirring at room temperature for 24 h. Afterward, octadecyltrimethoxysilane (22 μL, technical grade, 90%, Aldrich) was added. The mixture was stirred for another 24 h. The particles were then isolated by centrifugation, and washed several times with ethanol. Finally, these particles were redispersed in toluene to yield a homogeneous stock dispersion with a silica concentration of 1 g·mL^{-1}. The diameter of the nanoparticles was determined to be 50 ± 4 nm by counting 250 particles in the TEM image.

Synthesis of Hyperbranched Polyethoxysiloxane (PEOS). PEOS was synthesized according to a literature procedure.[24] The resulting PEOS product has following characteristics: degree of branching, 0.54; SiO_2 content, 49.2%; M_n, 1740 g mol^{-1}; and M_w/M_n, 1.9 (measured by gel permeation chromatography in chloroform with evaporative light scattering detector calibrated using polystyrene standards).

Preparation of Silica Colloidosomes. In a typical procedure, a silica nanoparticle dispersion (1 mL) was diluted with toluene (8.4 mL) and mixed with an HCl aqueous solution (1 mL, pH = 1). The mixture was emulsified by ultrasonic irradiation for 30 min (Branson Sonifier 450 cell disrupter, 3 mm microtip, 0.9 time circle, 247 W output). Afterward, a PEOS solution in toluene with a concentration of 0.2 g·mL^{-1} (0.6 mL) was added to the emulsion. The resulting mixture was gently stirred at room temperature for 3 days. The colloidosomes were isolated by centrifugation.

Electron Microscopy. Transmission electron microscopy (TEM) was performed on Zeiss Libra 120 TEM. The accelerating voltage was set at 120 kV. Scanning electron microscopy (SEM) was carried out on Hitachi S-4800 field-emission SEM. The samples were prepared by placing a drop of colloidosome dispersion in toluene on a Formvar-carbon-coated copper grid. Before being placed into the SEM or TEM specimen holder, the samples were air-dried under ambient conditions.

Thermogravimetric Analysis (TGA). TGA was performed on a NETZSCH TG 209c unit operating under nitrogen atmosphere with a flow rate of 10 mL·min^{-1}. After isolation using centrifuge

the colloidosomes were washed several times by *n*-hexane and then were kept in a loosely closed plastic centrifuge tube. After 1 week the smell of *n*-hexane completely disappeared, and then 10−15 mg of a sample were placed in a standard NETZSCH alumina 85 μL crucible for the measurement.

Fluorescence Microscopy. Fluorescence microscopy was performed on a Zeiss Axioplan 2 microscope equipped with XBO 75 illuminating system (Xenon lamp) and using a filter $\lambda_{ex} \geq 470$ nm and $\lambda_{em} \geq 500$ nm. Samples for the measurement were prepared following the same procedure as described above, but a portion of aqueous solution of tris(2,2′-bipyridyl) dichlororuthenium(II) hexahydrate (Ru(bpy)) (10 μL, 0.1 M) was added to every 1 mL of 0.1 M HCl solution.

FT-IR Spectroscopy. Before the measurement the colloidosome samples were dried at 60 °C overnight to remove the water. FT-IR spectra were then recorded on a Nicolet 60 SXR FT-IR spectrometer using KBr pellet technique.

Dye Release Test. Two water-soluble fluorescent dyes, Ru(bpy) and sulforhodamine B sodium salt, were dissolved in 0.1 M HCl solution, and the resulting 0.01 M dye solutions were used to prepare colloidosomes. The colloidosomes obtained in this way were placed into distilled water, and the system was gently stirred at room temperature. The water was monitored by fluorescence spectroscopy. During the test, the reaction vessels were always covered by an aluminum foil to avoid photobleaching.

Acknowledgment. We thank the research association Forschungskuratorium Textil e.V., Reinhardtstrasse 12 14, 10117 Berlin/D, for the financial support of the research project IGF-No. 333 ZN, which was provided within the promotion program of "Industrielle Gemeinschaftsforschung und −entwicklung (IGF)" from budget funds of the Federal Ministry of Economics and Technology (BMWi) due to a resolution of the German Bundestag *via* Arbeitsgemeinschaft industrieller Forschungsvereinigungen e.V.

REFERENCES AND NOTES

1. Binks, B. P.; Horozov, T. S. *Colloidal Particles at Liquid Interfaces*; Cambridge University Press: Cambridge, 2006.
2. Ramsden, W. Separation of Solids in the Surface-Layers of Solutions and 'Suspensions' (Observations on Surface-Membranes, Bubbles, Emulsions, and Mechanical Coagulation): Preliminary Account. *Proc. R. Soc. London* **1903,** *72*, 156–164.
3. Pickering, S. U. CXCVI.—Emulsions. *J. Chem. Soc., Trans* **1907,** *91*, 2001–2021.
4. Velev, O. D.; Furusawa, K.; Nagayama, K. Assembly of Latex Particles by Using Emulsion Droplets as Templates. 1. Microstructured Hollow Spheres. *Langmuir* **1996,** *12*), 2374–2384.
5. Dinsmore, A. D.; Hsu, M. F.; Nikolaides, M. G.; Marquez, M.; Bausch, A. R.; Weitz, D. A. Colloidosomes: Selectively Permeable Capsules Composed of Colloidal Particles. *Science* **2002,** *298*, 1006–1009.
6. Yow, H. N.; Routh, A. F. Release Profiles of Encapsulated Actives from Colloidosomes Sintered for Various Durations. *Langmuir* **2009,** *25*, 159–166.
7. Noble, P. F.; Cayre, O. J.; Alargova, R. G.; Velev, O. D.; Paunov, V. N. Fabrication of "Hairy" Colloidosomes with Shells of Polymeric Microrods. *J. Am. Chem. Soc.* **2004,** *126*, 8092–8093.
8. Duan, H.; Wang, D.; Sobal, N. S.; Giersig, M.; Kurth, D. G.; Mohwald, H. Magnetic Colloidosomes Derived from Nanoparticle Interfacial Self-Assembly. *Nano Lett.* **2005,** *5*, 949–952.
9. Croll, L. M.; Stöver, H. D. H. Formation of Tectocapsules by Assembly and Cross-Linking of Poly(divinylbenzene-alt-maleic anhydride) Spheres at the Oil−Water Interface. *Langmuir* **2003,** *19*, 5918–5922.
10. Thompson, K. L.; Armes, S. P.; Howse, J. R.; Ebbens, S.; Ahmad, I.; Zaidi, J. H.; York, D. W.; Burdis, J. A. Covalently Cross-Linked Colloidosomes. *Macromolecules* **2010,** *43*, 10466–10474.
11. Yuan, Q.; Cayre, O. J.; Fujii, S.; Armes, S. P.; Williams, R. A.; Biggs, S. Responsive Core−Shell Latex Particles as Colloidosome Microcapsule Membranes. *Langmuir* **2010,** *26*, 18408–18414.
12. Walsh, A.; Thompson, K. L.; Armes, S. P.; York, D. W. Polyamine-Functional Sterically Stabilized Latexes for Covalently Cross-Linkable Colloidosomes. *Langmuir* **2010,** *26*, 18039–18048.
13. Chen, T.; Colver, P. J.; Bon, S. A. F. Organic−Inorganic Hybrid Hollow Spheres Prepared from TiO_2-Stabilized Pickering Emulsion Polymerization. *Adv. Mater.* **2007,** *19*, 2286–2289.
14. Lin, Y.; Skaff, H.; Emrick, T.; Dinsmore, A. D.; Russell, T. P. Nanoparticle Assembly and Transport at Liquid−Liquid Interfaces. *Science* **2003,** *299*, 226–229.
15. Duan, H.; Wang, D.; Kurth, D. G.; Möhwald, H. Directing Self-Assembly of Nanoparticles at Water/Oil Interfaces. *Angew. Chem., Int. Ed.* **2004,** *43*, 5639–5642.
16. Binks, B. P.; Murakami, R. Phase Inversion of Particle-Stabilized Materials from Foams to Dry Water. *Nat. Mater.* **2006,** *5*, 865–869.
17. Ding, A.; Goedel, W. A. Experimental Investigation of Particle-Assisted Wetting. *J. Am. Chem. Soc.* **2006,** *128*, 4930–4931.
18. Pieranski, P. Two-Dimensional Interfacial Colloidal Crystals. *Phy. Rev. Lett.* **1980,** *45*, 569–573.
19. Kralchevsky, P.; Nagayama, K. *Particles at Fluid Interfaces and Membranes*; Elsevier Science B.V.: Amsterdam, The Netherlands, 2001.
20. Binks, B. P.; Clint, J. H. Solid Wettability from Surface Energy Components: Relevance to Pickering Emulsions. *Langmuir* **2002,** *18*, 1270–1273.
21. Goedel, W. A. A Simple Theory of Particle-Assisted Wetting. *Europhys. Lett.* **2003,** *62*, 607–613.
22. Lin, Y.; Böker, A.; Skaff, H.; Cookson, D.; Dinsmore, A. D.; Emrick, T.; Russell, T. P. Nanoparticle Assembly at Fluid Interfaces: Structure and Dynamics. *Langmuir* **2004,** *21*, 191–194.
23. Lee, D.; Weitz, D. A. Double Emulsion-Templated Nanoparticle Colloidosomes with Selective Permeability. *Adv. Mater.* **2008,** *20*, 3498–3503.
24. Zhu, X.; Jaumann, M.; Peter, K.; Möller, M.; Melian, C.; Adams-Buda, A.; Demco, D. E.; Blumich, B. One-Pot Synthesis of Hyperbranched Polyethoxysiloxanes. *Macromolecules* **2006,** *39*, 1701–1708.
25. Stöber, W.; Fink, A.; Bohn, E. Controlled Growth of Monodisperse Silica Spheres in the Micron Size Range. *J. Colloid Interface Sci.* **1968,** *26*, 62–69.
26. Murtagh, M. J.; Graham, E. K.; Pantano, C. G. Elastic Moduli of Silica Gels Prepared with Tetraethoxysilane. *J. Am. Ceram. Soc.* **1986,** *69*, 775–779.
27. Venditti, F.; Angelico, R.; Palazzo, G.; Colafemmina, G.; Ceglie, A.; Lopez, F. Preparation of Nanosize Silica in Reverse Micelles: Ethanol Produced during TEOS Hydrolysis Affects the Microemulsion Structure. *Langmuir* **2007,** *23*, 10063–10068.
28. McNamee, C. E.; Jaumann, M.; Möller, M.; Ding, A.; Hemeltjen, S.; Ebert, S.; Baumann, W.; Goedel, W. A. Formation of a Freely Suspended Membrane *via* a Combination of Interfacial Reaction and Wetting. *Langmuir* **2005,** *21*, 10475–10480.
29. Brinker, C.; Scherer, G. *Sol-Gel Science: The Physics and Chemistry of Sol-Gel Processing*; Academic Press: San Diego, CA, 1990.